JPn Neuroscience
The Journal of Physiology
J Physiol 593.17 (2015) pp 3849–3863

Osmosensation in TRPV2 dominant negative expressing skeletal muscle fibres

Nadège Zanou[1], Ludivine Mondin[1], Clarisse Fuster[2], François Seghers[1], Inès Dufour[1], Marie de Clippele[1], Olivier Schakman[1], Nicolas Tajeddine[1], Yuko Iwata[3], Shigeo Wakabayashi[3], Thomas Voets[4], Bruno Allard[2] and Philippe Gailly[1]

[1] *Laboratory of Cell Physiology, Institute of Neuroscience, Université catholique de Louvain, av. Mounier, B1.53.17, B-1200 Brussels, Belgium*
[2] *Centre de Génétique et de Physiologie Cellulaire et Moléculaire, Université Claude Bernard Lyon 1, CNRS, UMR 5534, 69622 Villeurbanne, France*
[3] *Department of Molecular Physiology, National Cardiovascular Center Research Institute Suita, Osaka 565–8565, Japan*
[4] *Laboratory of Ion Channel Research, Department of Cellular and Molecular Medicine, Katholiek Universiteit Leuven, B-3000 Leuven, Belgium*

Key points

- Increased plasma osmolarity induces intracellular water depletion and cell shrinkage (CS) followed by activation of a regulatory volume increase (RVI).
- In skeletal muscle, the hyperosmotic shock-induced CS is accompanied by a small membrane depolarization responsible for a release of Ca^{2+} from intracellular pools.
- Hyperosmotic shock also induces phosphorylation of STE20/SPS1-related proline/alanine-rich kinase (SPAK).
- TRPV2 dominant negative expressing fibres challenged with hyperosmotic shock present a slower membrane depolarization, a diminished Ca^{2+} response, a smaller RVI response, a decrease in SPAK phosphorylation and defective muscle function.
- We suggest that hyperosmotic shock induces TRPV2 activation, which accelerates muscle cell depolarization and allows the subsequent Ca^{2+} release from the sarcoplasmic reticulum, activation of the Na^+–K^+–Cl^- cotransporter by SPAK, and the RVI response.

Abstract Increased plasma osmolarity induces intracellular water depletion and cell shrinkage followed by activation of a regulatory volume increase (RVI). In skeletal muscle, this is accompanied by transverse tubule (TT) dilatation and by a membrane depolarization responsible for a release of Ca^{2+} from intracellular pools. We observed that both hyperosmotic shock-induced Ca^{2+} transients and RVI were inhibited by Gd^{3+}, ruthenium red and GsMTx4 toxin, three inhibitors of mechanosensitive ion channels. The response was also completely absent in muscle fibres overexpressing a non-permeant, dominant negative (DN) mutant of the transient receptor potential, V2 isoform (TRPV2) ion channel, suggesting the involvement of TRPV2 or of a TRP isoform susceptible to heterotetramerization with TRPV2. The release of Ca^{2+} induced by hyperosmotic shock was increased by cannabidiol, an activator of TRPV2, and decreased by tranilast, an inhibitor of TRPV2, suggesting a role for the TRPV2 channel itself. Hyperosmotic shock-induced membrane depolarization was impaired in TRPV2-DN fibres, suggesting that TRPV2 activation triggers the release of Ca^{2+} from the sarcoplasmic reticulum by depolarizing TTs. RVI requires the sequential activation of STE20/SPS1-related proline/alanine-rich kinase (SPAK) and NKCC1, a Na^+–K^+–Cl^- cotransporter, allowing ion entry and driving osmotic water flow. In fibres overexpressing TRPV2-DN as well as in fibres in which Ca^{2+} transients were abolished by the Ca^{2+} chelator BAPTA, the level of P-SPAK^{Ser373} in response to hyperosmotic shock was reduced, suggesting a modulation of SPAK phosphorylation by intracellular Ca^{2+}. We conclude that TRPV2

N. Zanou and L. Mondin contributed equally to this work.

DOI: 10.1113/JP270522

is involved in osmosensation in skeletal muscle fibres, acting in concert with P-SPAK-activated NKCC1.

(Received 12 March 2015; accepted after revision 19 June 2015; first published online 24 June 2015)
Corresponding author P. Gailly: Laboratory of Cell Physiology, Institute of Neuroscience, Université catholique de Louvain, av. Mounier, B1.53.17, B-1200 Brussels, Belgium. Email: philippe.gailly@uclouvain.be

Abbreviations 2-APB, 2-aminoethoxydiphenyl borate; CS, cell shrinkage; CTRL, control; DHPR, dihydropyridine receptor; di-8-ANNEPS, di-8-aminonaphtylethenylpyridinium; FDB, flexor digitorum brevis; GsMTx4 toxin, *Grammostola spatulata* toxin; NKCC1, Na^+–K^+–Cl^- cotransporter; OSR1, oxidative stress-responsive kinase 1; RVI, regulatory volume increase; RyR, ryanodine receptor; SFK-96365, 1-[β-[3-(4-methoxyphenyl) propoxy]-4-methoxyphenetyl]-1*H*-imidazole); SPAK, STE20/SPS1-related proline/alanine-rich kinase; TRPV2, transient receptor potential, V2 isoform; TRPV2-DN, dominant negative mutant of TRPV2; TT, transverse tubule; WNK protein kinase, with-no-K (lysine) protein kinase.

Introduction

Increased plasma osmolarity is observed in several physiological and pathological conditions such as food ingestion, exercise, hyperglycaemia and dehydration (Foster, 1974; Bratusch-Marrain & DeFronzo, 1983; Sjogaard *et al.* 1985; Haussinger *et al.* 1993; Watson *et al.* 1993). Hyperosmolarity induces intracellular water depletion and cell shrinkage (CS) followed by activation of a compensatory mechanism that restores cell volume, a process called regulatory volume increase (RVI).

The RVI subsequent to CS requires activation of NKCC1, a Na^+–K^+–Cl^- cotransporter, allowing ion entry and driving osmotic water flow (Sitdikov *et al.* 1989; Drewnowska & Baumgarten, 1991; Russell, 2000). In hyperosmotic conditions, activation of with-no-K (lysine) (WNK) protein kinase leads to the activation of STE20/SPS1-related proline/alanine-rich kinase (SPAK) and oxidative stress-responsive kinase 1 (OSR1) through phosphorylation of threonine/serine residues, which in turn phosphorylate and activate NKCC1 (Kahle *et al.* 2005; Richardson & Alessi, 2008).

Hyperosmolarity-induced CS and subsequent RVI occur in skeletal muscle. Due to its proportional mass in the body, skeletal muscle potentially plays an important role in whole body water balance. Its activity is also a source of perturbation. Indeed, intense exercise causes muscle to lose osmolytes such as lactate and K^+, which are released into the circulation. As a consequence of the increased blood osmolarity, non-contracting muscles lose water but the hyperosmolarity-induced NKCC1 activation counteracts the net loss of water from these cells and helps maintain their function (Gosmanov *et al.* 2003).

Related to the activation of the NKCC1 transporter in skeletal muscle, CS has been shown to induce a membrane depolarization of about 10–15 mV (van Mil *et al.* 1997; Geukes Foppen, 2004) and a subsequent increase in cytosolic Ca^{2+} concentration ($[Ca^{2+}]_i$) (Chawla *et al.* 2001; Wang *et al.* 2005; Weisleder & Ma, 2006; Martins *et al.* 2008).

The major source of Ca^{2+} in skeletal muscle is the Ca^{2+} released from the sarcoplamic reticulum (SR) (Clausen *et al.* 1979; Bruton, 1989). This is controlled by voltage-sensitive L-type channels, the dihydropyridine receptors (DHPRs), located in the transverse tubules (TTs). Through a conformational coupling, muscle depolarization leads to the opening of ryanodine receptor 1 (RyR1) and Ca^{2+} release from the SR (Melzer *et al.* 1995; Dulhunty 2006). If sufficient, increased cytosolic Ca^{2+} in response to electrical stimulation induces muscle cell contraction, a process named excitation–contraction coupling (Klein *et al.* 1996).

How muscle fibres sense osmotic changes and/or CS is not yet clear. It has been shown that hyperosmotic shock-induced CS is accompanied by transverse tubule (TT) dilatation (Apostol *et al.* 2009). WNK might constitute an osmosensor by itself (Zagorska *et al.* 2007), but the present study was designed to investigate the possible additional involvement of mechanosensitive channels, in particular channels belonging to the transient receptor potential (TRP) family.

The TRP channel superfamily constitutes a large and diverse class of proteins that are expressed in many tissues and cell types. This superfamily is composed by six subfamilies in mammals among which four have homology of structure in the transmembrane domains: classical (TRPC), vanilloid (TRPV), melastatin (TRPM) and ANKTM1 (TRPA). They are composed of six transmembrane domains, the pore being located between the fifth and the sixth domain. All subfamilies of TRP channels are permeable to cations and most of them to calcium with a ratio P_{Ca}/P_{Na} varying between 0.3 and 10 (Vassort & Fauconnier, 2008). Several TRP channels present mechanosensitive properties, including TRPC1 and TRPC6, TRPV2 and TRPV4, TRPM3, TRPA1 and TRPP2 (Arnadottir & Chalfie, 2010). Skeletal muscle expresses TRPC, TRPV and TRPM isoforms (Brinkmeier, 2011; Gailly, 2012). However, we previously showed that TRPC1 is not responsible for mechanosensitivity in skeletal muscle (Zanou *et al.* 2010). Several arguments

suggest a role of TRPV2 or TRPV4 in the detection of mechanical stimuli in skeletal muscle. Indeed, TRPV2, a Ca^{2+}-permeable channel simultaneously discovered by two groups (Caterina *et al.* 1999; Kanzaki *et al.* 1999), has been shown to constitute a component of osmotically sensitive cation channels in smooth muscle (Muraki *et al.* 2003). In skeletal muscle, it partially localizes in the intracellular membrane compartments but translocates to the plasma membrane when the membrane is stretched (Iwata *et al.* 2003). TRPV2 seems to be implicated in the pathophysiology of Duchenne muscular dystrophy. Indeed, in *mdx* mouse, a murine model of the disease, TRPV2 is mainly found in the plasma membrane where it constitutes an important Ca^{2+}-entry route leading to a sustained increase of $[Ca^{2+}]_i$ leading to muscle degeneration (Iwata *et al.* 2009). The entry of Ca^{2+} and/or Na^+ through TRPV2 also seems to be responsible of the characteristic sensitivity of dystrophic muscle to eccentric contraction (Zanou *et al.* 2009). Recently, TRPV4 was also demonstrated to contribute to mechanosensitivity in mouse skeletal muscle fibres (Ho *et al.* 2012).

As hypertonic challenge induces TT dilatation and cell depolarization, we investigated whether it could activate TRPV channels, contributing to Ca^{2+} and/or Na^+ entry and muscle cell depolarization. For this purpose, we investigated the response to hyperosmotic shock in normal muscle fibres and in muscle fibres expressing a dominant negative mutant of the TRPV2 channel (TRPV2-DN). Our results clearly show an impairment of osmosensation in TRPV2-DN cells. Indeed, these fibres presented a slower membrane depolarization, and loss of the Ca^{2+} transient and RVI in response to hyperosmotic shock. This was accompanied by a decrease in SPAK phosphorylation and defective muscle function. We suggest that TT dilatation in response to hyperosmotic shock induces TRPV2 activation, which accelerates muscle cell depolarization and allows the subsequent Ca^{2+} release from the SR, activation of NKCC1 and RVI.

Methods

Ethical approval

All the procedures used in this study were approved by the Animal Ethics Committee of the Université catholique de Louvain. A total of 52 C57BL6 male adult mice, among which were 18 TRPV2-DN mice, were deeply anaesthetized by intraperitoneal injection (10 ml kg^{-1}) of a solution containing ketamine (10 mg ml^{-1}) and xylazine (1 mg ml^{-1}) in order to preserve muscle perfusion during dissection. Depth of anaesthesia was assessed by the abolition of eyelid and pedal reflexes. After dissection, the animals were killed by cervical dislocation.

Generation of TRPV2-DN mice

Generation of TRPV2-DN transgenic mice expressing the haemagglutinin (HA)-tagged E604K mutant TRPV2 channel under the control of the α-skeletal actin promoter in skeletal muscle has been described previously (Iwata *et al.* 2009). All experiments were conducted on 12- to 16-week-old, sex-matched TRPV2-DN and their control mice.

Isolation of adult skeletal muscle fibres

The flexor digitorum brevis (FDB) muscles were incubated for 38 min at 37°C in an oxygenated 'Krebs-Hepes' solution (see composition below) containing 0.2% collagenase type IV (Sigma-Aldrich Corp., St Louis, MO, USA). Muscles were then washed twice in Dulbecco's modified Eagle's medium (DMEM)/HAM F12 (Sigma) supplemented with 2% fetal bovine serum (Sigma) and mechanically dissociated by repeated passages through fire-polished Pasteur pipettes of progressively decreasing diameter. Dissociated fibres were plated onto tissue culture dishes coated with Matrigel (BD Bioscience, San Jose, CA, USA) and allowed to adhere to the bottom of the dish for 2 h. For Ca^{2+} measurements, cells were plated on circular glass coverslips. Culture dishes were kept in an incubator, with 5% CO_2 at 30°C.

Measurements of cytosolic $[Ca^{2+}]$ and volume change

Muscle fibres were maintained in a Krebs-Hepes solution containing (mM): NaCl 135.5, $MgCl_2$ 1.2, KCl 5.9, glucose 11.5, Hepes 11.5, $CaCl_2$ 1.8 (pH 7.3, osmolarity adjusted to 310 mosmol l^{-1}). For some experiments, $CaCl_2$ was omitted and replaced by 200 μM Na-EGTA. Fibres were loaded for 1 h at room temperature with the membrane-permeant Ca^{2+}-indicator Fura-2/AM 1 μM. They were alternately excited (1 Hz) at 340 and 380 nm using a Lambda DG-4 ultra high speed wavelength switcher (Sutter Instrument, Novato, CA, USA) coupled to a Zeiss Axiovert 200 M inverted microscope (20× fluorescence objective) (Zeiss Belgium, Zaventem, Belgium). Images were acquired with a Zeiss Axiocam camera coupled to a 510 nm emission filter and analysed with the Axiovision software. Ca^{2+} concentration was evaluated from the ratio of fluorescence emission intensities excited at the two wavelengths using a calibration previously described (Vandebrouck *et al.* 2002). Fibre diameter was measured with Axiovision software. Fibres were submitted to a hyperosmotic shock by rapidly changing the normal Krebs solution to the same solution supplemented with 120 mM mannitol (osmolarity adjusted to 430 mosmol l^{-1}). Images were collected every 2 s for 4 min (during the diameter decrease) and thereafter every 30 s for 45 min. Diameter measurements (μm) were

performed on each fibre in the basal iso-osmotic (iso) condition (D_0), after 1 min (D_1) in hyperosmotic medium inducing a cell shrinkage (CS), and after 30 min (D_{30}), i.e. at the end of the RVI period. A relative volume recovery was then calculated as $(D_0 - D_{30})/(D_0 - D_1)$ expressed as a percentage.

Muscle fibre detubulation

Muscle fibres were detubulated using a procedure established by Kawai *et al.* (1999) on cardiac myocytes. Briefly, fibres were bathed for 15 min in a Krebs-Hepes solution made largely hypertonic with 1.5 M formamide. Cells were then rapidly returned to control Krebs-Hepes solution. In order to check the procedure, cells were labelled with di-8-aminonaphtylethenylpyridinium (di-8-ANNEPS, Molecular Probes) 2 μM for 2 min, rinsed three times, and imaged using 480 nm excitation light and detection at 640 nm. This procedure allowed us to keep detubulated fibres intact (no change in the morphology, fibres staying in a relaxed state, and $[Ca^{2+}]_i$ staying low). Measurements of cytosolic $[Ca^{2+}]$ using Fura-2 (see above) were performed on fibres not stained with di-8-ANNEPS to avoid any interference.

Electrophysiological experiments

Single fibres were current or voltage clamped using the silicone clamp technique as previously described (Pouvreau *et al.* 2007). Briefly, the major part of a single fibre was electrically insulated with silicone grease and a micropipette was inserted into the fibre through the silicone layer to current or voltage clamp the portion of the fibre free of grease (50–100 μm length) using a patch-clamp amplifier (Bio-Logic RK-400, Claix, France) in the whole-cell configuration. Command current pulse generation and data acquisition were done using the pCLAMP9 software (Axon Instruments Inc., USA) driving an A/D converter (Digidata 1322A, Axon Instruments). Analog compensation was systematically used to decrease the effective series resistance. Membrane voltages were acquired at a sampling frequency of 100 Hz. Cell capacitance was determined by integration of a current trace obtained with a 10 mV hyperpolarizing pulse from −80 mV in the voltage clamp configuration.

Muscle mechanics

Soleus muscles were dissected as mentioned above and were bathed in a 1 ml horizontal chamber continuously superfused with oxygenated Krebs solution (95% O_2–5% CO_2) containing (mM): NaCl 118, $NaHCO_3$ 25, KCl 5, KH_2PO_4 1, $CaCl_2$ 2.5, $MgSO_4$ 1, glucose 5, maintained at a temperature of 20 ± 0.1°C. One end of the muscle was tied to an isometric force transducer and the other end to an electromagnetic motor and length transducer. Stimulation was delivered through platinum electrodes running parallel to the muscles. Muscle length was carefully adjusted for maximal isometric force using 0.35 s maximally fused tetani. Force was recorded on a high-speed pen recorder (Sanborn model 320) and digitized at a sampling rate of 1 kHz with a peripheral component interconnect 6023E in/out card (National Instruments, Brussels, Belgium). Muscles were stimulated maximally for 300 ms at 125 Hz in isosmotic medium for 15 min to check the stability of force production in these conditions; then perfused medium was replaced by hypertonic medium and muscles were further stimulated for 45 min.

Western blot analysis

Soleus and FDB muscles were harvested, frozen in liquid nitrogen and kept at −80°C until use. Muscles were suspended in 500 μl lysis buffer containing (mM) Tris-HCl 50, EDTA 1, EGTA 1, β-glycerophosphate 10, KH_2PO_4 1, NaVO3 1, NaF 50, NaPPi 10, and a protease inhibitor cocktail containing (mg ml^{-1}) pancreas extract 0.02, pronase 0.005, thermolysin 0.0005, chymotrypsin 0.003 and papain 0.33 (Roche, Complete, Mini) and NP40 05%, homogenized with pipette tips for cells or Ultraturax for muscles (IKA-Labortechnik, Staufen, Germany) and incubated for 10 min at 4°C. Nuclei and unbroken cells were removed by centrifugation at 10,000 *g* for 10 min at 4°C. Samples were incubated with Laemli sample buffer containing SDS and β-mercaptoethanol for 3 min at 95°C and electrophoresed on 10% SDS-polyacrylamide gels, transferred on nitrocellulose membranes. Blots were incubated with rabbit anti-phospho-SPAK^{Ser373} and anti-GAPDH (Cell Signaling, Danvers, MA, USA) (1/1000 and 1/2000 respectively). After incubation with the secondary antibody (anti-rabbit IgG) coupled to peroxidase (Dako, Glostrup, Denmark), peroxidase was detected with ECL+ (Amersham, Diegem, Belgium) on ECL hyperfilm. Protein expression was quantified by densitometry.

Immunohistochemistry

Muscles were dissected, fixed in 4% paraformaldehyde on ice for 4 h, embedded in paraffin, and sectioned. Sections of 5 μm were deparaffinated, rehydrated and blocked using a 0.5% bovine serum albumin / 5% normal goat serum solution in phosphate buffered saline (PBS) during 1 h at room temperature. Sections were then incubated at 4°C overnight with rabbit anti-TRPV2 antibody PC 421 (1:20, Calbiochem, San Diego, CA, USA) or rabbit anti-HA tag antibody (1:800, Bethyl, Montgomery, TX, USA), both diluted in blocking solution. Primary antibodies

were detected by applying a goat anti-rabbit biotinylated second antibody (1:200, Vector Laboratories, Burlingame, CA, USA) for 2 h. Then, the sections were incubated in avidin–Texas red solution (1:100, Vector Laboratories, Burlingame, CA, USA) washed in PBS-BSA 2% solution and mounted in Vectashield (Vector Laboratories). Images were acquired using a 40× objective on a Zeiss S100 inverted microscope equipped with Axiocam camera.

Reagents

The GsMTx4 toxin, isolated from *Grammostola spatulata* spider (Suchyna *et al.* 2000), was obtained from PeptaNova (Sandhausen, Germany); SFK-96365 (1-[β-[3-(4-methoxyphenyl)propoxy]-4-methoxyphenetyl]-1 *H*-imidazole) from Alexis Corp. (Lausen, Switzerland); 2-aminoethoxydiphenyl borate (2-APB) from Alexis; Fura-2/AM from Invitrogen (Molecular Probes); and Tranilast and cannabidiol from Tocris (Bristol, UK). All other reagents were purchased from Sigma.

Statistics

Data are presented as means ± standard error of the mean (SEM). ANOVA or Student's *t* test was used to determine statistical significance except for membrane potential measurements for which a non-parametric analysis was used (the Kolmogorov–Smirnov test).

Results

Hyperosmotic shock induces a Ca^{2+} transient and a regulatory volume increase in skeletal muscle fibres

FDB muscle fibres were exposed to hyperosmotic medium (430 mosmol l^{-1} obtained by addition of mannitol) and fibre diameter and $[Ca^{2+}]_i$ were monitored. As shown in Fig. 1*A*, and quantified in Fig. 1*B*, hyperosmotic shock induced a rapid cell shrinkage (CS), with fibre diameter decreasing from 100 ± 5.4% to 89.4 ± 1.2%, followed

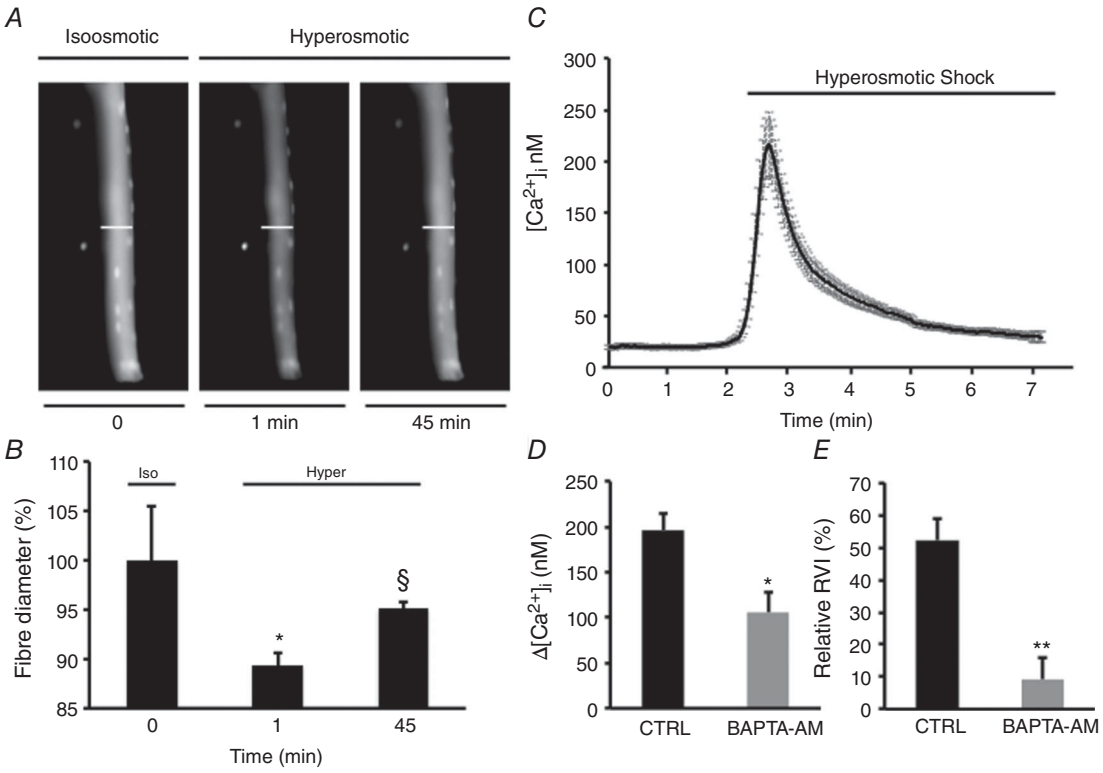

Figure 1. Hyperosmotic shock induces cell shrinkage and RVI accompanied by Ca^{2+} transient in muscle fibres
A, control (CTRL) fibres loaded with Fura-2 (excited at a wavelength of 380 nm and observed at 510 nm) and challenged with hyperosmotic medium (430 mosmol l^{-1} by addition of mannitol) exhibit a fast CS followed by a slow RVI. Bar represents 50 μm. *B*, quantification of data presented in A. Results expressed as means ± SEM, *P < 0.05 vs. iso; §P < 0.05 vs. CS; one-way ANOVA followed by Tukey's multicomparison test (n = 10). *C*, cytosolic Ca^{2+} transient induced by a hyperosmotic shock in CTRL fibres (mean ± SEM, n = 37). D and E, Ca^{2+} and RVI responses to hyperosmotic challenge in muscle fibres treated or not with BAPTA-AM and submitted to hyperosmotic shock. *D*, $\Delta[Ca^{2+}]$i is the difference between the peak amplitude and the resting $[Ca^{2+}]$i. *E*, relative RVI (expressed as a percentage) is calculated as the ratio $(D_0 - D_{30})/(D_0 - D_1)$, where D_0, D_1 and D_{30} are the diameters of fibres submerged in a hyperosmotic medium for 0, 1 and 30 min, respectively. *P < 0.05, **P < 0.01 vs. CTRL; Student's t test (n = 5).

by a long lasting regulatory volume increase (RVI), the diameter recovering to 95.1 ± 0.6% ($n = 16$, $P < 0.05$), corresponding to a relative recovery of 54%. This was accompanied by a transient $[Ca^{2+}]_i$ increase peaking at a maximal amplitude of 216 ± 30 nM ($n = 37$; Fig. 1*C*). Chelation of intracellular Ca^{2+} by BAPTA-AM decreased the amplitude of $[Ca^{2+}]_i$ in response to hyperosmolarity ($\Delta[Ca^{2+}]_i$, the difference between the peak amplitude and the resting $[Ca^{2+}]_i$, of 105 ± 22 nM compared to 172 ± 13 nM in control conditions ($n = 5$, $P < 0.05$; Fig. 1*D*) and, interestingly, prevented the RVI (relative recovery of only 6% compared to 54% in control fibres, $n = 5$, $P < 0.05$; Fig. 1*E*). These results suggest a role of Ca^{2+} in the RVI process.

Response to hyperosmotic shock was altered in TRPV2-DN expressing cells

To investigate whether mechanosensitive ion channels were involved in the mechanism of RVI, we treated muscle fibres with different inhibitors of these channels: Gd^{3+}, GsmTx4 toxin and ruthenium red (RR). In response to hyperosmotic shock, these treatments largely inhibited Ca^{2+} transients and the relative RVI (Fig. 2*A* and *B*), suggesting the participation of mechanosensitive channels in the process.

We therefore investigated osmosensation in muscle fibres overexpressing a dominant negative mutant form of TRPV2 (Iwata *et al.* 2009). Interestingly, hyperosmotic shock-induced Ca^{2+} transients were drastically inhibited in TRPV2-DN fibres compared to control fibres ($\Delta[Ca^{2+}]_i$ of 24 ± 3 nM, $n = 37$, *vs.* 196 ± 18 nM, $n = 29$, $P < 0.001$; Fig. 3*A* and *B*). In these fibres, RVI was abolished ($n = 8$, $P < 0.01$; Fig. 3*C*).

The osmosensor and/or its effectors are localized in transverse tubules

Results described above clearly point to a role of the TRPV2 ion channel in the hyperosmolarity-induced $[Ca^{2+}]_i$ transient and RVI. However, the source of Ca^{2+} was not identified. To test the extra- or intracellular origin of Ca^{2+}, we first investigated hyperosmotic response in a medium devoid of Ca^{2+} and found that muscle cells displayed similar Ca^{2+} response (data not shown), suggesting that Ca^{2+} is released from intracellular stores during the process. In skeletal muscle, the main intracellular source of Ca^{2+} is the SR, and Ca^{2+} release occurs upon cell depolarization, a process that involves a physical coupling between the DHPR present in transverse tubule (TT) membranes and RyR1 localized in the SR. We therefore detubulated muscle fibres and investigated the response to hyperosmotic shock. We checked by staining of the membranes with the lipophilic marker di-8-ANNEPS that TTs were indeed disconnected by the procedure (Fig. 4*A*). In these fibres, both Ca^{2+} response and RVI were almost abolished (Fig. 4*B* and *C*), suggesting the presence of the osmosensor and/or its effectors in the TTs.

These results prompted us to investigate the localization of TRPV2 in skeletal muscle cells. Immunostaining of TRPV2 using a TRPV2 antibody showed a striated pattern indicating the presence of TRPV2 in or near the TT and SR membranes (Fig. 5*A*). Using an anti-HA antibody, we also observed a striated staining pattern in cells overexpressing the HA–TRPV2-DN fusion protein. As expected, no staining was detected in control fibres (Fig. 5*B*).

We then treated muscle fibres with dantrolene, a specific inhibitor of Ca^{2+} release through RyR1 during excitation–contraction coupling in skeletal muscle. Ca^{2+} transients in these fibres were almost completely inhibited to 5.7 ± 2.5% ($n = 5$; $P < 0.001$), suggesting the requirement of muscle depolarization and excitation–contraction coupling

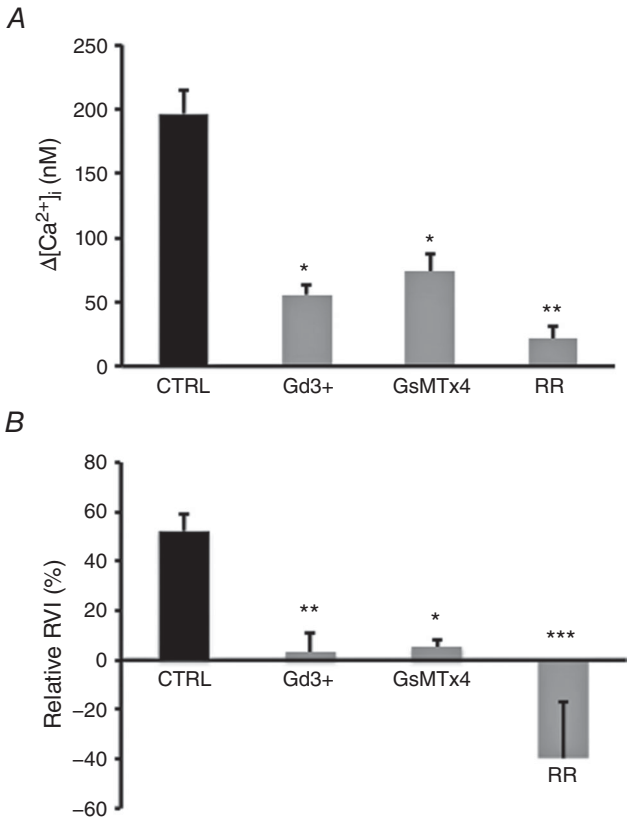

Figure 2. Modulation of Ca^{2+} transients and RVI by mechanosensitive channel inhibitors
$\Delta[Ca^{2+}]i$ (*A*) and relative RVI (*B*) in fibres pre-treated with 50 μm of $Gd^{3}+$ for 15 min, 5 μm of GsMTx4 toxin for 15 min and 40 μm of ruthenium red (RR) for 15 min. *P < 0.05, **P < 0.01 and ***P < 0.001 vs. CTRL; one-way ANOVA followed by Tukey's multicomparison test ($n = 5$).

during hyperosmolarity-induced Ca^{2+} release. Interestingly, tranilast, an inhibitor of TRPV2, decreased $[Ca^{2+}]_i$ transients by twofold and cannabidiol, an activator of TRPV2 potentiated the response by about threefold, the latter effect being largely inhibited by dantrolene and tranilast ($n \geq 5$ fibres in each condition, $P < 0.05$; Fig. 6).

TRPV2 participates in muscle cell depolarization during hyperosmotic shock

A series of electrophysiological experiments were performed in order to determine whether the strong reduction in the hyperosmotic shock-induced Ca^{2+} transients in TRPV2-DN muscle fibres resulted from an impaired depolarization of muscle fibres. At rest, measurement of the transmembrane current flowing in response to voltage pulses applied from −80 to −90 mV under voltage clamp conditions indicated that the mean resting membrane conductance was significantly higher in control fibres (295 ± 34 S F^{-1}, $n = 16$) as compared to TRPV2-DN fibres (135 ± 25 S F^{-1}, $n = 15$), suggesting that channels are partially open in these conditions. Figure 7 shows the mean changes in membrane potential induced by a hyperosmotic shock in TRPV2 control and TRPV2-DN current clamped fibres. On average TRPV2-DN fibres depolarized to a maximal voltage level of 10.8 ± 3 mV ($n = 11$), which was not significantly different from the voltage level of 9.7 ± 1.5 mV ($n = 15$) reached by the control fibres. However, hyperosmotic shock led to a rapid depolarization of control fibres while TRPV2-DN fibres were first slightly hyperpolarized and then depolarized at a much slower rate as compared to control fibres. It has to be noticed that in 4 out of 12 TRPV2-DN fibres tested, hyperpolarization was not followed by depolarization, whereas a depolarizing response was always observed in control fibres. A Kolmogorov–Smirnov test (a non-parametric test) was used to compare the changes in membrane potential as a function of time induced by mannitol in control and mutant fibres. All the fibres, including fibres that did not depolarize, were included in the data analysis. The Kolmogorov–Smirnov statistic quantifies a

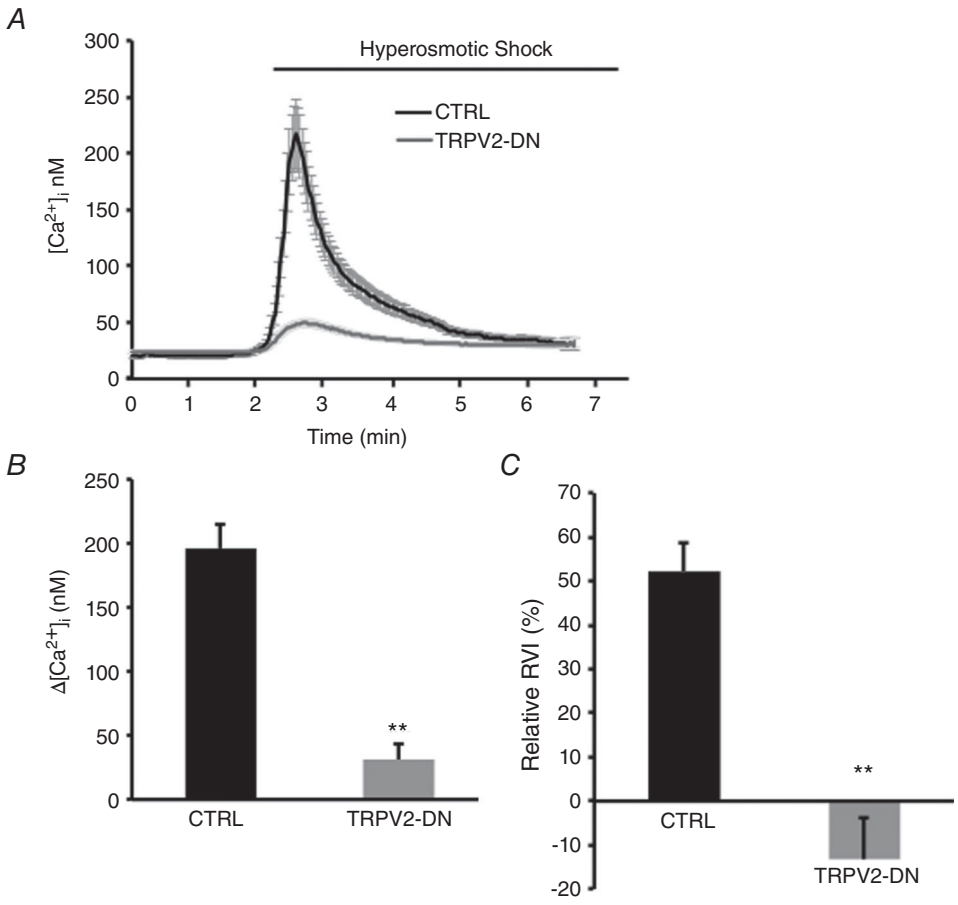

Figure 3. Ca^{2+} transients and RVI in control and TRPV2-DN fibres
Ca^{2+} transients (mean ± SEM) (*A*), quantification of Δ$[Ca^{2+}]$i (*B*) and relative RVI (*C*) in CTRL vs. TRPV2-DN fibres in response to hyperosmolarity. Results expressed as means ± SEM, **P < 0.01 vs. CTRL; Student's t test ($n \geq 8$).

distance between the empirical cumulative distribution functions of the two fibre populations. The results show that the distribution of the control cells significantly differs from that of the mutant cells ($D = 0.572$, $P < 0.0001$). NKCC1 has been reported to participate to hypertonic shock-induced depolarization. We therefore investigated whether the slow depolarization observed in TRPV2-DN fibres was sensitive to furosemide, an inhibitor of NKCC1. We observed that furosemide 500 μM reduced by 35 ± 5% the depolarization induced by the hyperosmotic shock in TRPV2-DN fibres ($n = 9$).

NKCC1 cotransporter activation is impaired in TRPV2-DN expressing cells

NKCC1 is a key player in the RVI process, allowing Na^+, K^+ and 2 Cl^- entry into the cell, which is accompanied by osmotic water movement. It has been reported that WNK constitutes an osmosensor that activates NKCC1 through the intermediate activation of SPAK and OSR1 (Vitari *et al.* 2005, 2006; Rafiqi *et al.* 2010; Grimm *et al.* 2012). Interestingly, the phosphorylation of SPAK on both threonine (P-SPAK^{Thr233}) and serine (P-SPAK^{Ser373}) residues is well correlated with the activation of NKCC1 (Sid *et al.* 2010). We therefore indirectly investigated the activity of NKCC1 by quantifying by imunoblot the phosphorylation time course of SPAK on serine 373 residue. A progressive phosphorylation of SPAK^{Ser373} was observed in response to hyperosmotic shock in both soleus (slow twitch) and FDB (mixed fast and slow twitch) muscles, peaking after 5 and 10 min, respectively (Fig. 8*A*). To investigate whether the phosphorylation of SPAK was Ca^{2+} dependent, we measured hyperosmolarity-induced P-SPAK^{Ser373} in control muscles pre-treated or not with BAPTA-AM for 3 h. Interestingly, we observed a drastic decrease in P-SPAK^{Ser373} in those muscles compared to their control ones (Fig. 8*B*), indicating a modulation of SPAK phosphorylation by intracellular Ca^{2+}. In TRPV2-DN expressing cells, the level of P-SPAK^{Ser373} in response to hyperosmotic shock was reduced to 40.3 ± 13.3% in soleus and to 17.8 ± 5.4% in FDB muscles in comparison to control muscles ($n = 6$, $P < 0.05$; Fig. 9*A* and *B*), suggesting an involvement of TRPV2 in the process.

Defect of force production in TRPV2-DN expressing muscle fibres exposed to hyperosmotic shock

The role of RVI in muscle function is still unknown. We therefore measured force production during

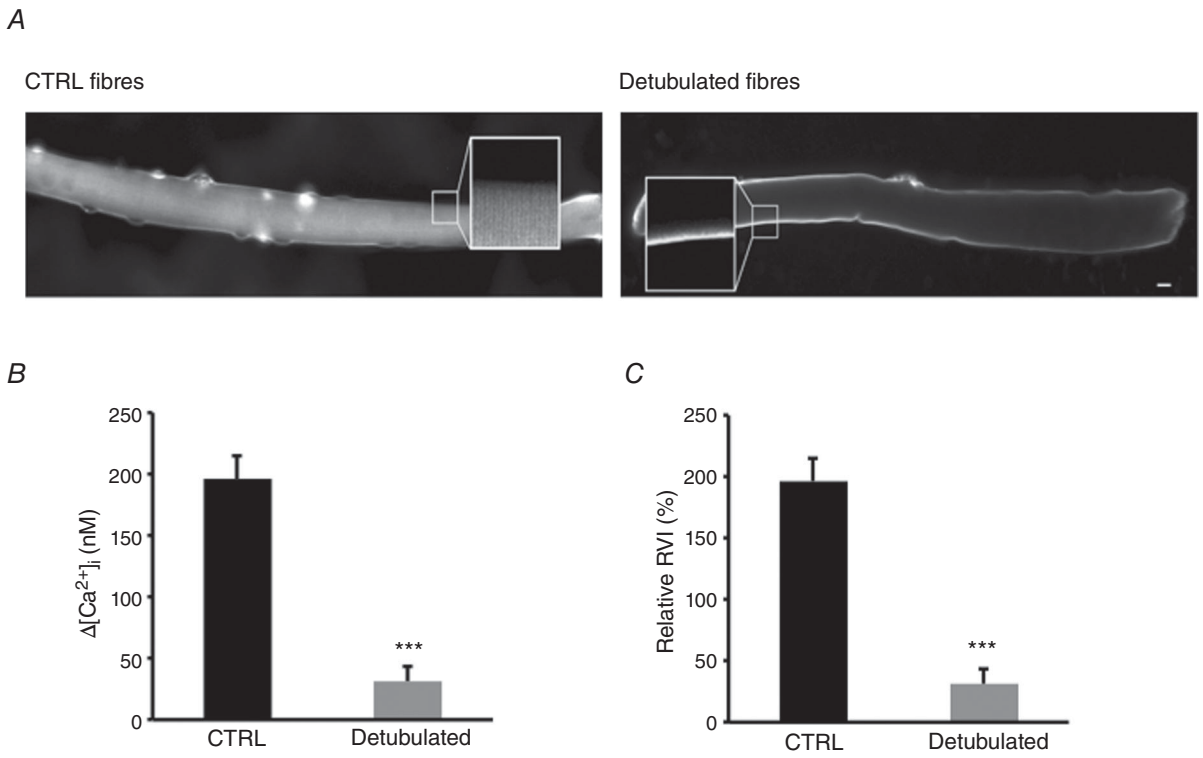

Figure 4. [Ca^{2+}]i and RVI responses in detubulated fibres
A, control or detubulated isolated muscle fibres are stained with 2 μm di-ANNEPS for 2 min. Bar represents 10 μm. *B*, Δ[Ca^{2+}]i response and (*C*) relative RVI after hyperosmotic shock in CTRL fibres and detubulated fibres. Results expressed as means ± SEM, **P < 0.01, ***P < 0.001 vs. non-detubulated CTRL; Student's t test ($n = 6$).

hyperosmotic shock. Soleus muscles were stimulated maximally every 3 min in isoosmotic medium for 15 min to verify the stability of force production in these conditions and for 45 min in a hyperosmotic medium. Isoosmotic medium did not alter muscle force production under tested conditions either in control or in TRPV2-DN muscles. Hyperosmotic challenge induced a rapid force drop to a similar level in control and TRPV2-DN muscles (20% of first tetanus). Interestingly, this was accompanied by a long lasting force recovery in control muscles whereas TRPV2-DN muscles did not recover ($n = 6$, $P < 0.05$; Fig. 10).

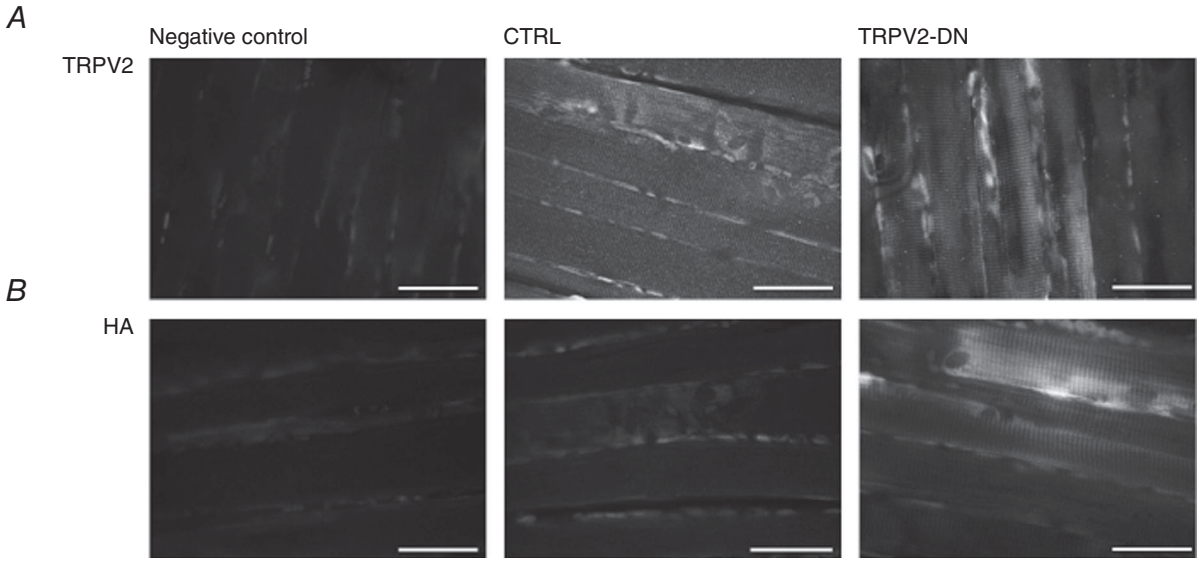

Figure 5. Localization of TRPV2 in muscle fibres
Immunohistochemistry of TRPV2 (*A*) and HA tag in CTRL and TRPV2-DN expressing fibres using anti-TRPV2 and anti-HA antibodies. Negative control corresponds to staining without the primary antibody (but with the secondary antibody). Representative images of three different stainings. Bar represents 50 μm.

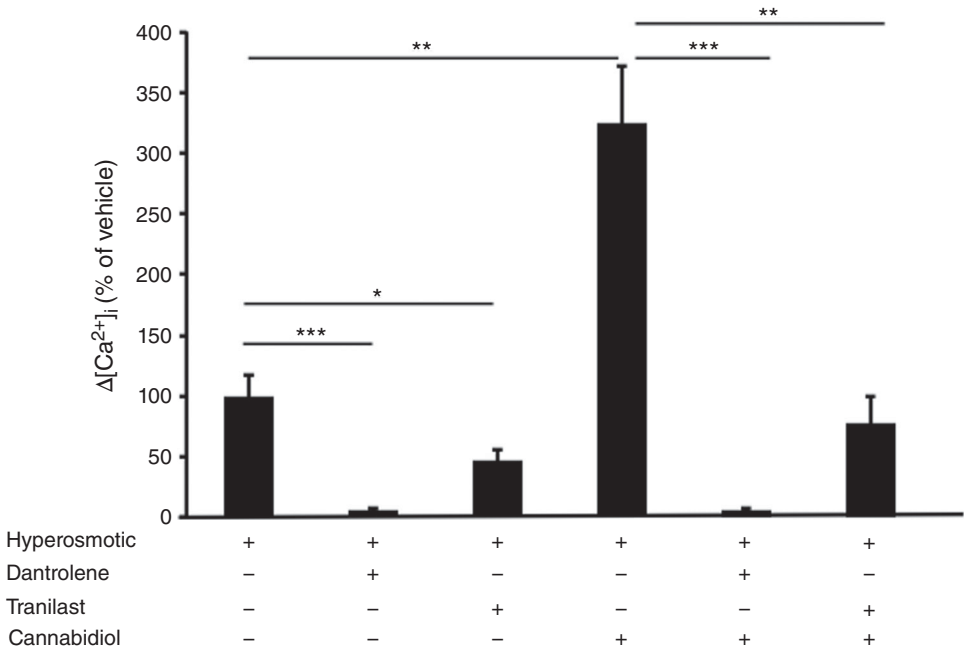

Figure 6. Modulation of Ca^{2+} responses to hyperosmotic shock in fibres treated with vehicle or dantrolene 30 μm for 10 min, with tranilast 100 μm for 15 min or with cannabidiol 10 μm for 5 min
Results are expressed as a percentage of $[Ca^{2+}]$i peak observed in the presence of the vehicle. *P < 0.05, **P < 0.01, ***P < 0.001 vs. CTRL non-treated fibres; two-way ANOVA followed by Tukey's multicomparison test ($n \geq 5$).

Discussion

In skeletal muscle, hyperosmolarity-induced cell shrinkage activates NKCC1, which allows Na^+, K^+ and Cl^- influx into the cell. Consequently, osmolytes are retained within the cell and volume can recover (Gosmanov *et al.* 2003). This is accompanied by a transient increase in $[Ca^{2+}]_i$ inside the cell. If the role of Ca^{2+} in the mechanisms of regulatory volume decrease (RVD) is well established, Ca^{2+}-induced RVI has not been thoroughly investigated (Chawla *et al.* 2001; Hoffmann & Hougaard, 2001; Wehner *et al.* 2003; Martins *et al.* 2008). Besides, the sources of $[Ca^{2+}]_i$ transients observed during the RVD and the RVI processes are different and the possible link between $[Ca^{2+}]_i$ increase and the RVI process has not been elucidated (Marino & La Spada,

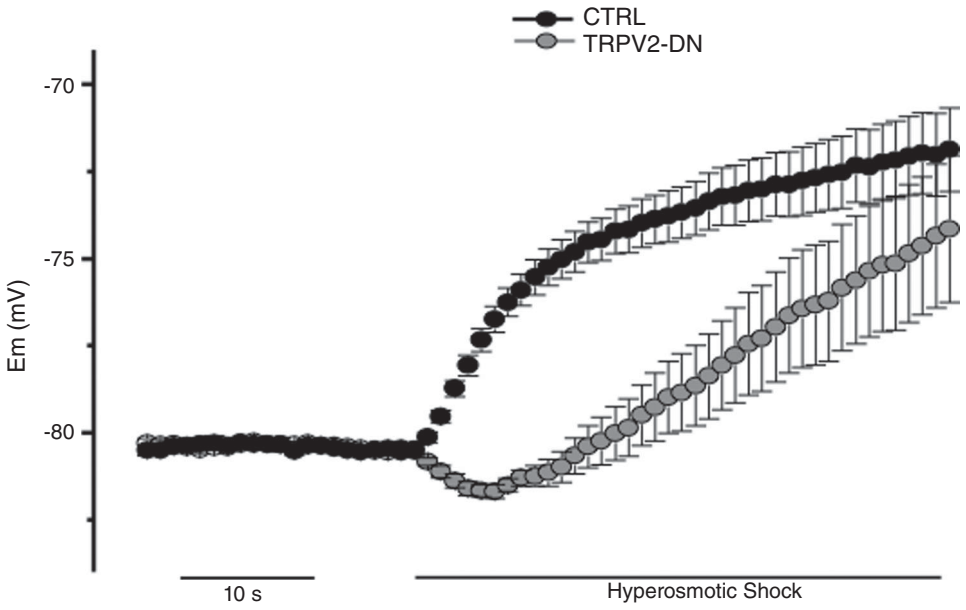

Figure 7. Effects of a hyperosmotic shock on membrane potential in CTRL and TRPV2-DN fibres
Muscle fibres were current clamped using the silicone clamp method and resting membrane potential was brought to −80 mV by injection of a constant negative current. Each data point corresponds to the mean membrane potential recorded every second in 16 TRPV2 and 12 TRPV2-DN fibres.

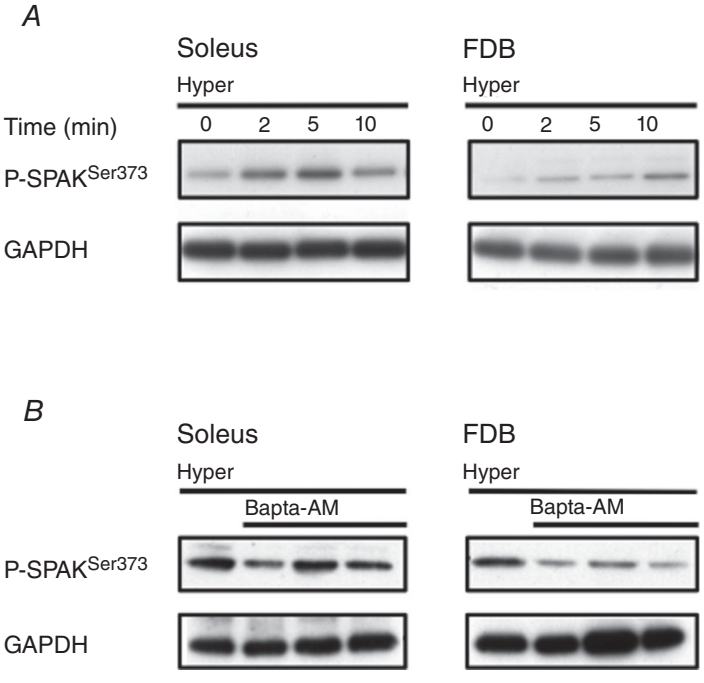

Figure 8. Modulation of P-SPAK^{Ser373} by BAPTA-AM
A, immunoblot showing the time course of P-SPAK^{Ser373} in soleus and FDB muscles from CTRL mice incubated in iso- (0 min) and hyperosmotic solutions (2, 5 and 10 min). *B*, P-SPAK^{Ser373} measured in muscle fibres pre-treated or not for 3 h with BAPTA-AM (30 μm, 3 examples presented, from 3 different mice) and challenged with hyperosmotic medium during 5 min (soleus) and 10 min (FDB). GAPDH was used as a loading control.

2007; Wormser *et al.* 2011). Some studies have indicated that the $[Ca^{2+}]_i$ increase in response to hyperosmolarity is due to NKCC1 activity, which allows membrane depolarization (van Mil *et al.* 1997; Geukes Foppen, 2004; Hattori & Wang, 2006; Pickering *et al.* 2009).

In the present study, different observations indicate that hyperosmotic shock activates the TRPV2 channel, which induces membrane depolarization, which in turn triggers Ca^{2+} release from SR stores. First, Ca^{2+} release from the SR was abolished by dantrolene, an inhibitor of depolarization-induced RyR1 opening, suggesting that the release of Ca^{2+} induced by hypertonic stimulation essentially results from membrane depolarization (Ellis & Bryant, 1972; Ellis & Carpenter, 1972; Ikemoto *et al.* 2001; Szentesi *et al.* 2001; Zhao *et al.* 2001). Second, the response also decreased after pretreatment of the fibres with RR, GsmTx4 and Gd^{3+}, suggesting an involvement of a TRPV channel. The response was almost abolished in fibres expressing TRPV2-DN, implicating the TRPV2 channel itself or a channel able to multimerize with the TRPV2-DN isoform. Note that the TRPV4 channel was recently shown to contribute to muscle mechanosensitivity (Ho *et al.* 2012); we cannot exclude that it may heteromultimerize with TRPV2. Third, Ca^{2+} release was increased after pretreatment with cannabidiol and decreased after pretreatment with tranilast, pointing to

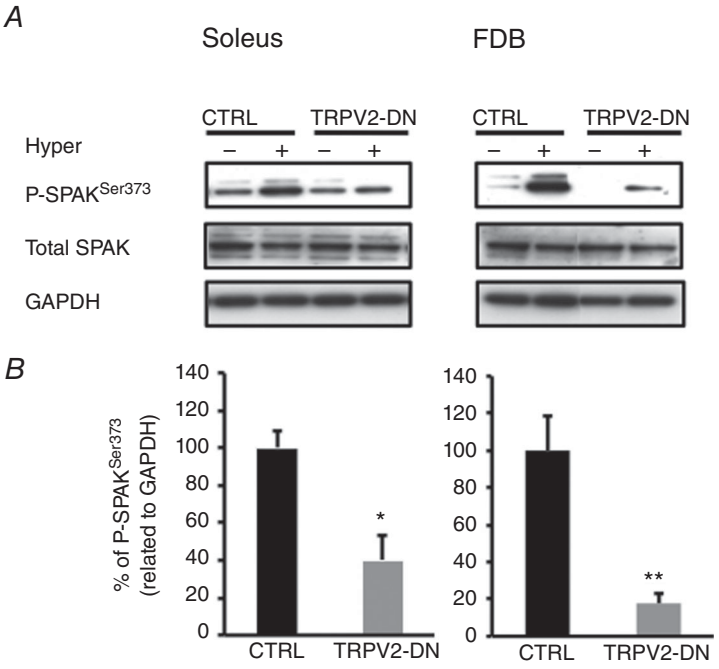

Figure 9. Modulation of P-SPAK^{Ser373} in TRPV2-DN muscles
A, immunoblot showing P-SPAK^{Ser373} in TRPV2-DN soleus and FDB muscles submitted 5 and 10 min, respectively, to hyperosmotic shock. GAPDH was used as a loading control. *B*, quantification of P-SPAK^{Ser373} in CTRL and TRPV2-DN muscles submitted to hyperosmotic shock. *P < 0.05 vs. CTRL; Student's t test ($n = 6$).

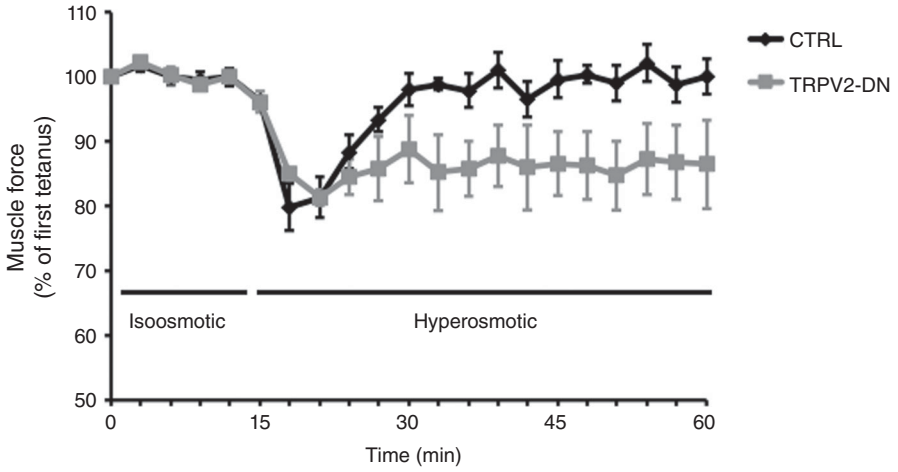

Figure 10. Muscle force production under hyperosmotic shock
Soleus muscles from CTRL and TRPV2-DN mice were maximally stimulated every 3 min for 15 min in isoosmotic solution and for 45 min in hyperosmotic solution. *P < 0.05 vs. CTRL, one-way repeated measure ANOVA ($n = 6$).

a role of TRPV2 itself. Fourth, control cells showed a rapid depolarization in response to hyperosmolarity that was impaired in TRPV2-DN. Interestingly, in these cells a depolarization was still observed, but it occurs at a slower rate rendering it inefficient in triggering EC coupling. The slow residual depolarization might be due, as mentioned above, to NKCC1 activation itself, as it is partially inhibited by furosemide, but also to other mechanisms such as a decrease in K^+ permeability (Van Mil *et al.* 1997). We observed that the TRPV2 ion channel is localized in or near the TTs. We therefore suggest that TRPV2 might be activated directly or indirectly by membrane stretch when TTs are dilated in response to osmotically driven cell shrinkage (Apostol *et al.* 2009).

Activation of NKCC1 upon hypertonic challenge involves the activation of WNK, which phosphorylates SPAK and OSR1, which in turn phosphorylate and activate NKCC1 (Richardson & Alessi, 2008). The present paper shows that the phosphorylation of SPAK is largely dependent on $[Ca^{2+}]_i$ increase. Indeed, in the presence of the Ca^{2+} chelator BAPTA or in TRPV2-DN fibres that do not increase their $[Ca^{2+}]_i$ in response to a hyperosmotic challenge, SPAK stayed less phosphorylated, and as a consequence RVI did not occur. We therefore conclude that TRPV2 channels participate in the depolarization induced by the hypertonic challenge and that the consecutive increase in $[Ca^{2+}]_i$ controls SPAK activation and RVI. A second pathway activating NKCC1 is the PKC/ERK axis in response to agonists or EGF stimulation. Crosstalk between the WNK/SPAK/OSR1 and PKC/ERK pathways has been described. Indeed, phosphorylation of NKCC1 by SPAK and OSR1 kinase may operate downstream of ERK (Kahle *et al.* 2010). Moreover, EGF and/or agonist-mediated PKC/ERK activation and NKCC1 phosphorylation are described as a Ca^{2+}-dependent process (Wang *et al.* 2011). This pathway seems to be involved in the response to hyperosmolarity in tracheal epithelial cells (Liedtke & Cole, 2002), suggesting a role of Ca^{2+}-dependent PKC/ERK activation in SPAK/OSR1 phosphorylation and NKCC1 activation during hyperosmotic shock. Another Ca^{2+}-dependent pathway that can modulate NKCC1 activity involves calcium-binding protein 39 (Cab39), a scaffolding protein distantly related to armadillo proteins that facilitates the activation (T-loop phosphorylation) of SPAK/OSR1 and consequently of NKCC1 without WNK involvement (Ponce-Coria *et al.* 2012). In either of these cases, the SPAK/OSR1 axis seems important for Ca^{2+}-mediated NKCC1 activation. Thus, in hyperosmotic conditions, TRPV2-mediated intracellular Ca^{2+} increase may directly or indirectly control SPAK/OSR1 phosphorylation and NKCC1 activation.

Control muscles submitted to a hyperosmotic shock presented a rapid force drop that recovered after a period of about 12 min. TRPV2-DN muscles presented a similar force drop, but did not recover after a period of up to 45 min. Such force drop has been previously attributed to three phenomena (Hermsmeyer *et al.* 1972; Wildenthal *et al.* 1975; Willerson *et al.* 1975; Gulati & Babu, 1986): (i) decreased muscle fibre volume induces a restriction of contractile apparatus space that makes difficult the interaction between actin and myosin filaments; (ii) cell depolarization maintains muscle in a refractory period that prevents contractile response upon stimulations; and (iii) the increase in intracellular ion concentration alters actin and myosin cross bridges. The two latter hypotheses are unlikely since (i) depolarization observed in TRPV2-DN fibres is slower and weaker than that observed in control fibres; and (ii) control muscles reached normal force a few minutes later despite the maintenance of the hypertonic medium, excluding a direct role of ionic concentration increase in the alteration of force development. We therefore propose that muscle force drop in response to hyperosmotic shock is related to spatial hindrance. In agreement with this hypothesis, control muscles that recovered cell volume also recovered muscle force.

In conclusion, our results show that TRPV2 is involved in osmosensation in skeletal muscle fibres, acting in concert with P-SPAK-activated NKCC1. Dysregulation of osmosensation observed in TRPV2-DN mice has deleterious consequences on skeletal muscle function but could also alter whole body water balance during pathological processes such as dehydration.

References

Apostol S, Ursu D, Lehmann-Horn F & Melzer W (2009). Local calcium signals induced by hyper-osmotic stress in mammalian skeletal muscle cells. *J Muscle Res Cell Motil* **30**, 97–109.

Arnadottir J & Chalfie M (2010). Eukaryotic mechanosensitive channels. *Annu Rev Biophys* **39**, 111–137.

Bratusch-Marrain PR & DeFronzo RA (1983). Impairment of insulin-mediated glucose metabolism by hyperosmolality in man. *Diabetes* **32**, 1028–1034.

Brinkmeier H (2011). TRP channels in skeletal muscle: gene expression, function and implications for disease. *Adv Exp Med Biol* **704**, 749–758.

Bruton JD (1989). Role of chloride in hypertonicity-induced contractures of rat soleus muscle. *Q J Exp Physiol* **74**, 565–567.

Caterina MJ, Rosen TA, Tominaga M, Brake AJ & Julius D (1999). A capsaicin-receptor homologue with a high threshold for noxious heat. *Nature* **398**, 436–441.

Chawla S, Skepper JN, Hockaday AR & Huang CL (2001). Calcium waves induced by hypertonic solutions in intact frog skeletal muscle fibres. *J Physiol* **536**, 351–359.

Clausen T, Dahl-Hansen AB & Elbrink J (1979). The effect of hyperosmolarity and insulin on resting tension and calcium fluxes in rat soleus muscle. *J Physiol* **292**, 505–526.

Drewnowska K & Baumgarten CM (1991). Regulation of cellular volume in rabbit ventricular myocytes: bumetanide, chlorothiazide, and ouabain. *Am J Physiol Cell Physiol* **260**, C122–131.

Dulhunty AF (2006). Excitation-contraction coupling from the 1950 s into the new millennium. *Clin Exp Pharmacol Physiol* **33**, 763–772.

Ellis KO & Bryant SH (1972). Excitation-contraction uncoupling in skeletal muscle by dantrolene sodium. *NaunynSchmiedebergsArch Pharmacol* **274**, 107–109.

Ellis KO & Carpenter JF (1972). Studies on the mechanism of action of dantrolene sodium. A skeletal muscle relaxant. *NaunynSchmiedebergsArch Pharmacol* **275**, 83–94.

Foster DW (1974). Insulin deficiency and hyperosmolar coma. *Adv Intern Med* **19**, 159–173.

Gailly P (2012). TRP channels in normal and dystrophic skeletal muscle. *Curr Opin Pharmacol* **12**, 326–334.

Geukes Foppen RJ (2004). In skeletal muscle the relaxation of the resting membrane potential induced by K^+ permeability changes depends on Cl^- transport. *Pflugers Archiv* **447**, 416–425.

Gevaert T, Vriens J, Segal A, Everaerts W, Roskams T, Talavera K, Owsianik G, Liedtke W, Daelemans D, Dewachter I, VanLeuven F, Voets T, DeRidder D & Nilius B (2007). Deletion of the transient receptor potential cation channel TRPV4 impairs murine bladder voiding. *J Clin Invest* **117**, 3453–3462.

Gosmanov AR, Lindinger MI & Thomason DB (2003). Riding the tides: K^+ concentration and volume regulation by muscle Na^+-K^+-$2Cl^-$ cotransport activity. *News Physiol Sci* **18**, 196–200.

Grimm PR, Taneja TK, Liu J, Coleman R, Chen YY, Delpire E, Wade JB & Welling PA (2012). SPAK isoforms and OSR1 regulate sodium-chloride co-transporters in a nephron-specific manner. *J Biol Chem* **287**, 37673–37690.

Gulati J & Babu A (1986). Kinetics of force redevelopment in isolated intact frog fibers in solutions of varied osmolarity. *Biophys J* **49**, 949–955.

Hattori T & Wang PL (2006). Involvement of Na^+-K^+-$2Cl^-$ cotransporters in hypertonicity-induced rise in intracellular calcium concentration. *Int J Neurosci* **116**, 1501–1507.

Haussinger D, Roth E, Lang F & Gerok W (1993). Cellular hydration state: an important determinant of protein catabolism in health and disease. *Lancet* **341**, 1330–1332.

Hermsmeyer K, Rulon R & Sperelakis N (1972). Loss of the plateau of the cardiac action potential in hypertonic solutions. *J Gen Physiol* **59**, 779–793.

Ho TC, Horn NA, Huynh T, Kelava L & Lansman JB (2012). Evidence TRPV4 contributes to mechanosensitive ion channels in mouse skeletal muscle fibers. *Channels (Austin)* **6**, 246–254.

Hoffmann EK & Hougaard C (2001). Intracellular signalling involved in activation of the volume-sensitive K^+ current in Ehrlich ascites tumour cells. *Comp Biochem Physiol A Mol Integr Physiol* **130**, 355–366.

Ikemoto T, Hosoya T, Aoyama H, Kihara Y, Suzuki M & Endo M (2001). Effects of dantrolene and its derivatives on Ca^{2+} release from the sarcoplasmic reticulum of mouse skeletal muscle fibres. *Br J Pharmacol* **134**, 729–736.

Iwata Y, Katanosaka Y, Arai Y, Komamura K, Miyatake K & Shigekawa M (2003). A novel mechanism of myocyte degeneration involving the Ca^{2+}-permeable growth factor-regulated channel. *J Cell Biol* **161**, 957–967.

Iwata Y, Katanosaka Y, Arai Y, Shigekawa M & Wakabayashi S (2009). Dominant-negative inhibition of Ca^{2+} influx via TRPV2 ameliorates muscular dystrophy in animal models. *Hum Mol Genet* **18**, 824–834.

Kahle KT, Rinehart J, de Los Heros P, Louvi A, Meade P, Vazquez N, Hebert SC, Gamba G, Gimenez I & Lifton RP (2005). WNK3 modulates transport of Cl^- in and out of cells: implications for control of cell volume and neuronal excitability. *Proc Natl Acad Sci U S A* **102**, 16783–16788.

Kahle KT, Rinehart J & Lifton RP (2010). Phosphoregulation of the Na-K-2Cl and K-Cl cotransporters by the WNK kinases. *Biochim Biophys Acta* **1802**, 1150–1158.

Kanzaki M, Zhang YQ, Mashima H, Li L, Shibata H & Kojima I (1999). Translocation of a calcium-permeable cation channel induced by insulin-like growth factor-I. *Nat Cell Biol* **1**, 165–170.

Kawai M, Hussain M & Orchard CH (1999). Excitation-contraction coupling in rat ventricular myocytes after formamide-induced detubulation. *Am J Physiol Heart Circ Physiol* **277**, H603–609.

Klein MG, Cheng H, Santana LF, Jiang YH, Lederer WJ & Schneider MF (1996). Two mechanisms of quantized calcium release in skeletal muscle. *Nature* **379**, 455–458.

Liedtke CM & Cole TS (2002). Activation of NKCC1 by hyperosmotic stress in human tracheal epithelial cells involves PKC-δ and ERK. *Biochim Biophys Acta* **1589**, 77–88.

Liedtke W & Friedman JM (2003). Abnormal osmotic regulation in trpv4$^{-/-}$ mice. *Proc Natl Acad Sci U S A* **100**, 13698–13703.

Marino A & LaSpada G (2007). Calcium and cytoskeleton signaling during cell volume regulation in isolated nematocytes of *Aiptasia mutabilis* (Cnidaria: Anthozoa). *Comp Biochem Physiol A Mol Integr Physiol* **147**, 196–204.

Martins AS, Shkryl VM, Nowycky MC & Shirokova N (2008). Reactive oxygen species contribute to Ca^{2+} signals produced by osmotic stress in mouse skeletal muscle fibres. *J Physiol* **586**, 197–210.

Melzer W, Herrmann-Frank A & Luttgau HC (1995). The role of Ca^{2+} ions in excitation-contraction coupling of skeletal muscle fibres. *Biochim Biophys Acta* **1241**, 59–116.

Muraki K, Iwata Y, Katanosaka Y, Ito T, Ohya S, Shigekawa M & Imaizumi Y (2003). TRPV2 is a component of osmotically sensitive cation channels in murine aortic myocytes. *Circ Res* **93**, 829–838.

Pickering JD, White E, Duke AM & Steele DS (2009). DHPR activation underlies SR Ca^{2+} release induced by osmotic stress in isolated rat skeletal muscle fibers. *J Gen Physiol* **133**, 511–524.

Ponce-Coria J, Gagnon KB & Delpire E (2012). Calcium-binding protein 39 facilitates molecular interaction between Ste20p proline alanine-rich kinase and oxidative stress response 1 monomers. *Am J Physiol Cell Physiol* **303**, C1198–1205.

Pouvreau S, Collet C, Allard B & Jacquemond V (2007). Whole-cell voltage clamp on skeletal muscle fibers with the silicone-clamp technique. *Methods Mol Biol* **403**, 185–194.

Rafiqi FH, Zuber AM, Glover M, Richardson C, Fleming S, Jovanovic S, Jovanovic A, O'Shaughnessy KM & Alessi DR (2010). Role of the WNK-activated SPAK kinase in regulating blood pressure. *EMBO Mol Med* **2**, 63–75.

Richardson C & Alessi DR (2008). The regulation of salt transport and blood pressure by the WNK-SPAK/OSR1 signalling pathway. *J Cell Sci* **121**, 3293–3304.

Russell JM (2000). Sodium-potassium-chloride cotransport. *Physiol Rev* **80**, 211–276.

Sid B, Miranda L, Vertommen D, Viollet B & Rider MH (2010). Stimulation of human and mouse erythrocyte Na^+-K^+-$2Cl^-$ cotransport by osmotic shrinkage does not involve AMP-activated protein kinase, but is associated with STE20/SPS1-related proline/alanine-rich kinase activation. *J Physiol* **588**, 2315–2328.

Sitdikov RF, Urazaev A, Volkov EM, Poletaev GI & Khamitov Kh S (1989). [Effects of hyperosmolarity and furosemide on resting membrane potentials and skeletal muscle fiber volume in rats]. *Biulleten' eksperimental'noi biologii i meditsiny* **108**, 563–566. For translation: http://link.springer.com/article/10.1007%2FBF00839691.

Sjogaard G, Adams RP & Saltin B (1985). Water and ion shifts in skeletal muscle of humans with intense dynamic knee extension. *Am J PhysiolRegulIntegrComp Physiol* **248**, R190–196.

Suchyna TM, Johnson JH, Hamer K, Leykam JF, Gage DA, Clemo HF, Baumgarten CM & Sachs F (2000). Identification of a peptide toxin from *Grammostola spatulata* spider venom that blocks cation-selective stretch-activated channels. *J Gen Physiol* **115**, 583–598.

Szentesi P, Collet C, Sarkozi S, Szegedi C, Jona I, Jacquemond V, Kovacs L & Csernoch L (2001). Effects of dantrolene on steps of excitation-contraction coupling in mammalian skeletal muscle fibers. *J Gen Physiol* **118**, 355–375.

vanMil HG, Geukes Foppen RJ & Siegenbeek van Heukelom J (1997). The influence of bumetanide on the membrane potential of mouse skeletal muscle cells in isotonic and hypertonic media. *Br J Pharmacol* **120**, 39–44.

Vandebrouck C, Martin D, Colson-Van Schoor M, Debaix H & Gailly P (2002). Involvement of TRPC in the abnormal calcium influx observed in dystrophic (mdx) mouse skeletal muscle fibers. *J Cell Biol* **158**, 1089–1096.

Vassort G & Fauconnier J (2008). Transient receptor potential, TRP channels: a new family of channels broadly expressed. *M S-Med Sci* **24**, 163–168.

Vitari AC, Deak M, Morrice NA & Alessi DR (2005). The WNK1 and WNK4 protein kinases that are mutated in Gordon's hypertension syndrome phosphorylate and activate SPAK and OSR1 protein kinases. *BiochemJ* **391**, 17–24.

Vitari AC, Thastrup J, Rafiqi FH, Deak M, Morrice NA, Karlsson HK & Alessi DR (2006). Functional interactions of the SPAK/OSR1 kinases with their upstream activator WNK1 and downstream substrate NKCC1. *BiochemJ* **397**, 223–231.

Wang X, Weisleder N, Collet C, Zhou J, Chu Y, Hirata Y, Zhao X, Pan Z, Brotto M, Cheng H & Ma J (2005). Uncontrolled calcium sparks act as a dystrophic signal for mammalian skeletal muscle. *Nat Cell Biol* **7**, 525–530.

Wang Z, Bildin VN, Yang H, Capo-Aponte JE, Yang Y & Reinach PS (2011). Dependence of corneal epithelial cell proliferation on modulation of interactions between ERK1/2 and NKCC1. *Cell Physiol Biochem* **28**, 703–714.

Watson PD, Garner RP & Ward DS (1993). Water uptake in stimulated cat skeletal muscle. *Am J PhysiolRegulIntegrComp Physiol* **264**, R790–796.

Wehner F, Olsen H, Tinel H, Kinne-Saffran E & Kinne RK (2003). Cell volume regulation: osmolytes, osmolyte transport, and signal transduction. *Rev Physiol Biochem Pharmacol* **148**, 1–80.

Weisleder N & Ma JJ (2006). Ca^{2+} sparks as a plastic signal for skeletal muscle health, aging, and dystrophy. *Acta Pharmacol Sin* **27**, 791–798.

Wildenthal K, Adcock RC, Crie JS, Templeton GH & Willerson JT (1975). Negative inotropic influence of hyperosmotic solutions on cardiac muscle. *Am J Physiol* **229**, 1505–1509.

Willerson JT, Crie JS, Adcock RC, Templeton GH & Wildenthal K (1975). Importance of calcium in the inotropic effect of hyperosomotic agents, norepinephrine, paired electrical stimulation, and treppe. *Recent Adv Stud Cardiac Struct Metab* **8**, 219–232.

Wormser C, Mason LZ, Helm EM & Light DB (2011). Regulatory volume response following hypotonic stress in Atlantic salmon erythrocytes. *Fish Physiol Biochem* **37**, 745–759.

Zagorska A, Pozo-Guisado E, Boudeau J, Vitari AC, Rafiqi FH, Thastrup J, Deak M, Campbell DG, Morrice NA, Prescott AR & Alessi DR (2007). Regulation of activity and localization of the WNK1 protein kinase by hyperosmotic stress. *J Cell Biol* **176**, 89–100.

Zanou N, Iwata Y, Schakman O, Lebacq J, Wakabayashi S & Gailly P (2009). Essential role of TRPV2 ion channel in the sensitivity of dystrophic muscle to eccentric contractions. *FEBS Lett* **583**, 3600–3604.

Zanou N, Shapovalov G, Louis M, Tajeddine N, Gallo C, Van Schoor M, Anguish I, Cao ML, Schakman O, Dietrich A, Lebacq J, Ruegg U, Roulet E, Birnbaumer L & Gailly P (2010). Role of TRPC1 channel in skeletal muscle function. *Am J Physiol Cell Physiol* **298**, C149–C162.

Zhao F, Li P, Chen SR, Louis CF & Fruen BR (2001). Dantrolene inhibition of ryanodine receptor Ca^{2+} release channels. Molecular mechanism and isoform selectivity. *J Biol Chem* **276**, 13810–13816.

Additional information

Competing interests

The authors declare no competing financial interests.

Authors contribution

N.Z., L.M, B.A. and P.G. designed experiments, performed experiments, interpreted data and wrote the paper. C.F., F.S.,

I.D., O.S., performed experiments and interpreted data. N.T., Y.I., S.W. and T.V. critically revised the manuscript. All authors were involved in writing the paper and in the final approval of the manuscript for publication. Experiments were done in the Laboratory of Cell Physiology of the Université catholique de Louvain and at the Centre de Génétique et de Physiologie Cellulaire et Moléculaire, Université Claude Bernard Lyon 1.

Funding

The work was funded by the "Association française contre les myopathies" (AFM grant 16738), the "Association belge contre les maladies neuro-musculaires" (ABMM), by a Concerted Research Action from the General Direction of Scientific Research of the French Community of Belgium (ARC 10/15-029) and the Interuniversity Poles of Attraction Belgian Science Policy (P7/13). L.M. was post-doctoral fellow and N.Z. is postdoctoral researcher of the Fonds de la Recherche Scientifique (FNRS, Belgium).

Acknowledgements

L.M. was a post-doctoral fellow and N.Z. is a postdoctoral researcher of the Fonds de la Recherche Scientifique (FNRS, Belgium).